

Research on Film Damage Image Classification Based on Improved VGG16

Huilin Zhang^{1,a*}, Mingxuan Zhang^{1,b}, Xiaohui Su^{1,c}, and Shuping Xu^{1,d}

¹School of Computer Science and Engineering Xi'an Technological University Xi'an, China

^a748512736@qq.com, ^b3572213105@qq.com, ^c287099144@qq.com, ^d563937848@qq.com

Abstract. In this paper, an improved convolutional neural network based on VGG16 network model is proposed to solve the problems of whether the film image is damaged by the traditional method and the difficulty and low accuracy of the damage type. Use migration learning to prevent over-fitting due to a small number of data sets; The fusion of cross entropy loss function and center loss function can optimize multiple targets at the same time to get more accurate results. In order to effectively prevent the gradient explosion and the gradient disappear and accelerate the training speed of the network; the improved network model is called the BN-VGG16 network model. The data sets of four kinds of damage types, including crack, dehumidification, particle and scratch, were constructed by means of image shooting, random rotation, stretching and migration. The improved BN-VGG16 network model is trained and tested on the data set. The experimental results show that the recognition accuracy of BN-VGG16 for film image damage category can reach 77%. Compared with other models, this model has obvious advantages in recognition accuracy.

Keywords: VGG16; Convolution neural network Migration learning; Multi-loss function fusion BN layer

1. Introduction

Optical thin films refer to films coated on the surface of some optical devices or other components. Modern optical instruments utilize a large number of coated optical elements. Under the influence of strong lasers, damage to optical elements is almost inevitable, and once an optical element is damaged, it will affect the normal operation of the entire system. In order for optical systems to operate stably for a long time, optical components need frequent replacement, which greatly increases costs. Therefore, improving the laser damage resistance of optical thin films is of great significance to optical systems. Accurately determining whether a thin film is damaged is a key factor in the precise measurement of LIDT (Laser Induced Damage Threshold). LIDT measures the laser damage resistance of optical thin films. Only by accurately measuring the laser damage resistance can researchers explore methods to improve it from multiple perspectives, thereby reducing the operating costs of optical systems.

Currently, there are many methods to detect whether thin films are damaged, such as: plasma flash method, acousto-optic method, scattered light intensity measurement method, photothermal deflection method, and microscope observation method. Each method has its own advantages and disadvantages and is suitable for different detection scenarios. Among them, the microscope observation method is prescribed by international standards, and its detection results have a certain accuracy, but overall detection efficiency is low. The image method is an improvement of the microscope observation method. As a traceability method of the international standard ISO 11254, it has the advantages of simple operation and low cost.

With the continuous development of artificial intelligence technology, machine learning and deep learning have been widely used in image recognition, speech recognition, and many other fields, achieving breakthrough progress. Therefore, how to apply machine learning and deep learning technologies to image classification research has become a new hot spot. In recent years, deep convolutional neural networks and other machine learning concepts have been gradually applied to defect detection classification research at home and abroad. However, most focus on the classification of steel surface defects and pipeline characteristics/defects, while research on the classification of thin film surface defects is still rare. With the explosive development of machine learning and deep learning research, numerous image classification networks have emerged, such as AlexNet, VGGNet, ResNet, DenseNet, etc.. These deep learning methods can independently extract

useful features from massive data and recognize images. In practical applications, utilizing existing pre-trained models for transfer learning is a common model training method, which significantly improves recognition accuracy and shortens training time.

This paper constructs 4 types of thin film damage image datasets and carries out research on a thin film damage image classification method based on the improved VGG16 model. In the VGG16 network model, pre-trained weights based on the ImageNet dataset are introduced for transfer training. Multi-loss function fusion is utilized, a BN layer is added after each convolutional layer, and the network structure is optimized by fine-tuning model parameters. The goal is to improve the model's recognition accuracy, achieve fast and accurate classification of thin film damage images, and lay a theoretical foundation and technical support for further enhancing the laser resistance of optical thin films.

2. Construction of film damage image data set

2.1 Image acquisition.

The experiment uses a digital microscope with its own CCD imaging system to capture and store images. To obtain color images of the thin film samples under a bright field, a halogen lamp with uniform illumination is used as a reflective illumination source below the sample stage. This experiment obtained four damage types of organic thin film images in a bright field environment. These four damage types are Crack, Dewetting, Particle, and Scratch. Among them, there are 24,740 crack images, 23,320 dewetting images, 7,650 particle images, and 6,490 scratch images, totaling 62,200 images.

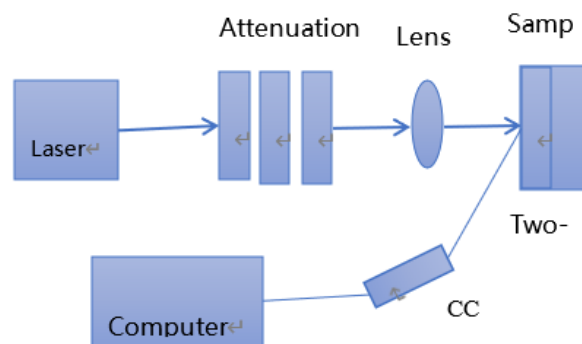
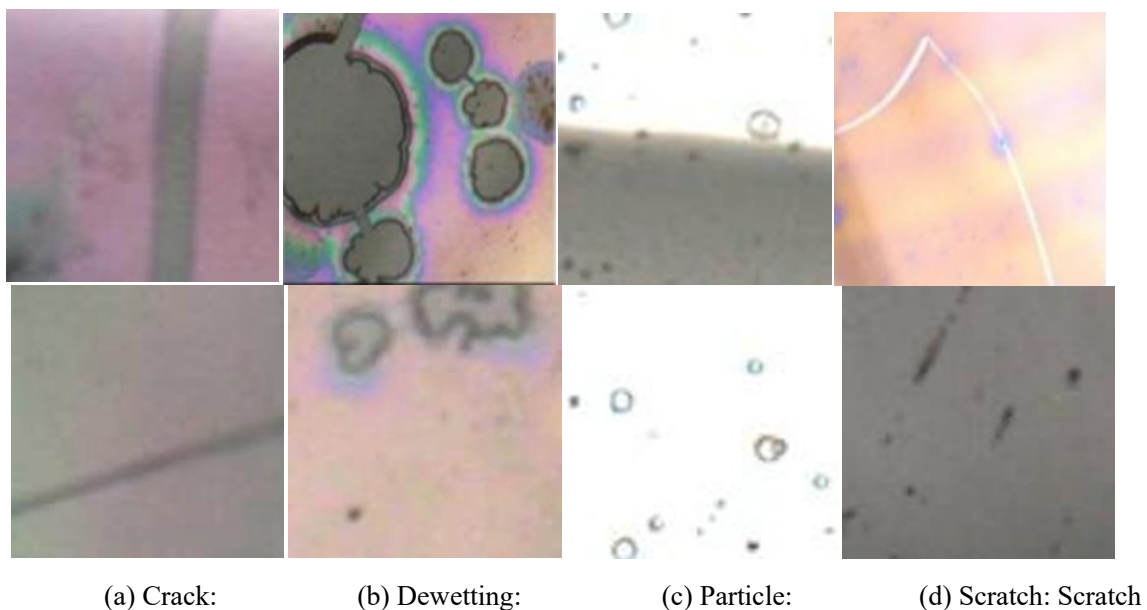


Figure 1. Experimental Device Diagram



(a) Crack:

(b) Dewetting:

(c) Particle:

(d) Scratch: Scratch

Figure 2. Film Damage Types

2.2 Image preprocessing.

Some images contain noise and other interference. To eliminate irrelevant information in the image, restore truly useful information, and improve the generalization ability of the model, the obtained images need to be preprocessed. The main preprocessing steps are as follows: (1) Image scaling. VGG16 requires the input image size to be $224 \times 224 \times 3$, so the acquired images are scaled to this size to adapt to model training. (2) Filtering and denoising. The main role is to suppress image noise as much as possible while retaining image detail information. This paper compares the effect of four common filtering and denoising methods on thin film damage images from the perspective of Mean Squared Error (MSE) and Peak Signal-to-Noise Ratio (PSNR).

Table 1 Comparison Of Four Filter Denoising Methods

	MAE(Mean absolute error)	PSNR(Peak signal-to-noise ratio)
Gaussian high-pass filtering	122.62364477040816	6.190143180037355
Gaussian low pass filtering	24.150211256377553	54.066039976495624
Median filtering	49.43827726403061	47.9103296244559
Arithmetic mean filtering	39.48865991709184	51.16036123693778

As can be seen from Table 1, the use of low-pass Gaussian filtering has the smallest MSE and the largest PSNR. Therefore, to reduce the interference of random noise, low-pass Gaussian filtering is selected for denoising before feature extraction.

(3) Edge extraction. Using edge detection algorithms to extract image features can effectively remove redundant information in the image, offering certain advantages for improving classification accuracy. This experiment compares four common edge extraction methods.

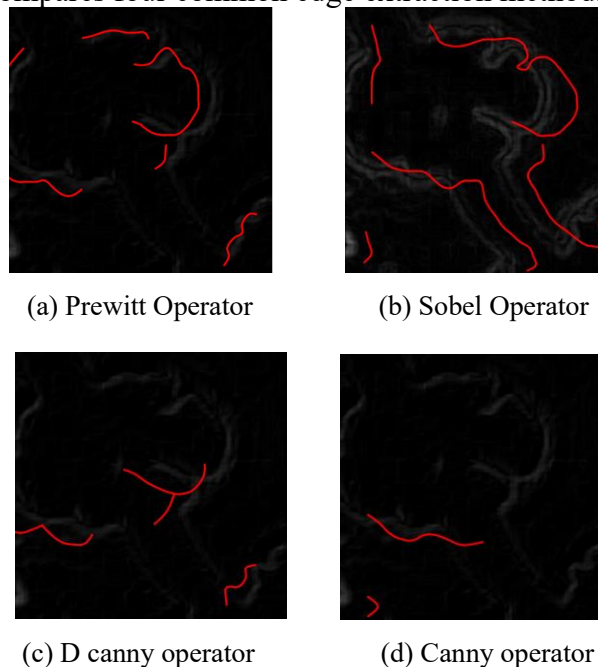


Figure 3. Edge Extraction Effect of four kinds of Damaged Images

From the effect diagrams of the four edge detection algorithms, the LoG operator and Canny operator basically completely smooth out the edge information and detail information in the image during the detection process. The Sobel operator detects clearer edges for thin film damage images than the Prewitt operator. Therefore, the Sobel operator is a more suitable edge detection method in this experiment. (4) Data augmentation. This paper divides the original dataset into a training set

(49,760 images), a validation set (6,220 images), and a test set (6,220 images) at a ratio of 8:1:1. Data augmentation is applied only to the training set accounting for 80%, not the validation and test sets. This paper selects 4 image transformation techniques (rotation, translation, shear, and scaling) to augment the images in the training set 7 times, resulting in a total of 348,320 images in the final training set.

2.3 Dataset Construction.

All original images are numbered, classified, and labeled (Label 1 for Crack, Label 2 for Dewetting, Label 3 for Particle, Label 4 for Scratch). Finally, all images are imported into the computer in jpg format to complete the construction of the 4 types of thin film damage image database. All images in this database serve as the input dataset for the BN-VGG16 convolutional neural network, and images in the training, validation, and test sets are randomly extracted by the computer.

3. Membrane Damage Classification Model Based on Improved VGG16

3.1 Convolution Neural Network and VGG16.

VGGNet won 2nd place in the 2014 ImageNet image classification competition, and VGG16 is one of the best-performing networks in the VGGNet family. Compared with the latest network structures, VGG16 has a simple structure without complex bottleneck designs. The model only contains very small (3×3) convolutional filters, and the network mainly includes convolutional layers, pooling layers, and fully connected layers.

3.2 Construction of BN-VGG16 Convolution Neural Network Model.

Because the original VGG16 network model still has defects such as low classification accuracy and excessively long training time when classifying thin film damage images, this paper improves the original network model. Based on the original model, transfer learning, multi-loss function fusion, and a BN layer added after each convolutional layer are utilized to construct the improved BN-VGG16 network model. Transfer learning can use pre-trained model parameters from others to train our smaller dataset and achieve good results. Multi-loss function fusion can simultaneously optimize multiple objectives, thereby making the thin film damage classification results more accurate. The BN layer can prevent gradient explosion and vanishing, accelerate network training and convergence speeds, reduce training time, and make the model more stable.

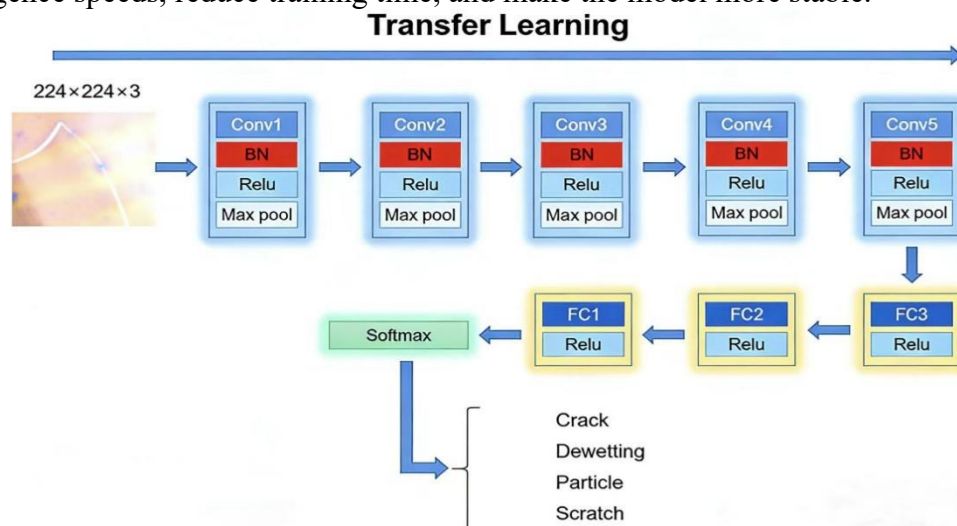


Figure 4. BN-VGG16 Network Model Diagram

1) Transfer learning.

When a network is relatively large (with many parameters) and the dataset size is small, it is insufficient to train the entire network, leading to overfitting and extremely poor training results. However, using transfer learning, pre-trained model parameters can be used to train a smaller dataset and still achieve good results. Therefore, this study uses weights pre-trained on the ImageNet dataset for training the thin film damage dataset. The ImageNet dataset contains over one

million images across 1,000 categories. Although it does not contain thin film damage images, the determination of thin film damage types relies mainly on contours and other features; thus, transfer learning via the ImageNet dataset is viable.

2) Multi-loss function fusion.

In traditional neural network training, usually only one loss function (such as cross-entropy loss) is used, but this often ignores other important information in the network, resulting in inaccurate final results. Therefore, multi-loss function fusion is proposed to solve this problem. The advantage is that it can optimize multiple objectives simultaneously, achieving more accurate results. It can also expand the inter-class distance and reduce the intra-class distance of thin film damage images, further improving classification accuracy.

The cross-entropy cost function is often used in classification tasks and controls the overall trend of the model. The definition is as follows:

$$c = - \sum_{x=1}^n [y \log \hat{y} + (1-y) \log(1-\hat{y})] \quad (1)$$

where n is the number of batch samples, x is the input, y is the label value, and \hat{y} represents the actual output

The advantage of the center loss function is that it can learn features with a smaller intra-class distance, thereby reducing intra-class differences and increasing inter-class differences to a certain extent, thus improving classification accuracy. The definition is as follows:

$$L_c = \frac{1}{2} \sum_{i=1}^n \|x_i - C_{y_i}\|_2^2 \quad (2)$$

where n is the number of batch samples, x_i denotes the i -th feature of class y_i , and C_{y_i} represents the center value of the i -th class feature.

The cross-entropy loss function and the center loss function are fused and extended to a multi-layer neural network. Assuming the expected values of the output neurons are $y = \{y_1, y_2, y_3, \dots\}$ and $\hat{y} = \{\hat{y}_1^L, \hat{y}_2^L, \hat{y}_3^L, \dots\}$, the fused calculation formula is as follows:

$$L = C + \alpha L_c = - \sum_{x=1}^n [y \log \hat{y}_x + (1-y) \log(1-\hat{y}_x)] + \frac{\alpha}{2} \sum_{i=1}^n \|x_i - C_{y_i}\|_2^2 \quad (3)$$

Where the fusion coefficient α ranges from 0 to 1. Through multi-loss function fusion, the inter-class distance of thin film damage is enlarged, the intra-class distance is reduced, network convergence is accelerated, and classification efficiency and accuracy are further improved.

BN layer. The original VGG16 model does not have a BN layer. The BN layer normalizes the data distribution before the activation function receives the input. The specific calculation is mean removal and normalization, standardizing data distribution to a standard normal distribution, making the input value of the activation function fall in a more sensitive region (where the gradient is larger). This prevents gradient explosion and vanishing, accelerates network training, reduces training time, and makes the model more stable. Therefore, BN is usually placed before the activation function. In the BN-VGG16 model, the BN layer is added after every convolutional layer and before the activation function of the original VGG16 model.

The BN layer needs to compute the mean μ and variance σ of all elements in a minibatch input feature (x_i), then subtract the mean from x_i and divide by the standard deviation, and finally perform an affine transformation using learnable parameters γ and β to obtain the final BN output y_i . The specific process is as follows:

Input: Values of x over a mini-batch : $\beta = \{x_i, \dots, m\}$;
Parameters to be learned: $\gamma \beta$
Output: $\{y_i = BN_{\gamma, \beta}(x_i)\}$

$$\mu_B \leftarrow \frac{1}{m} \sum_{i=1}^m x_i \quad //\text{mini-batch mean}$$

$$\sigma_B^2 \leftarrow \frac{1}{m} \sum_{i=1}^m (x_i - \mu_B)^2 \quad //\text{mini-batch variance}$$

$$\hat{x}_i \leftarrow \frac{x_i - \mu_B}{\sqrt{\sigma_B^2 + \varepsilon}} \quad //\text{normalize}$$

$$y_i \leftarrow \gamma \hat{x}_i + \beta \equiv BN_{\gamma, \beta}(x_i) \quad //\text{scale and shift}$$

he specific process is: 1) Calculate the sample mean; 2) Calculate sample variance; 3) Standardization of sample data; 4) Translate and zoom processing: Introduce and two parameters to train and two parameters, and introduce the releasable reconstruction parameter sum, so that our network can learn to restore the feature distribution to be learned by the original network.

Two learnable parameters γ and β are introduced for training. These learnable reconstruction parameters γ and β allow the network to recover the original feature distribution when necessary, while retaining the normalization effect to stabilize training and accelerate convergence.

4. Experimental results and analysis

This experiment primarily utilizes a self-made thin film damage image dataset and the ImageNet image dataset. Accuracy and recognition time are selected as the main evaluation indicators of the network model. Model memory usage and parameter count are also comprehensively considered to facilitate future embedded development. Precision, accuracy, recall, and F-score are calculated using a confusion matrix to comprehensively evaluate the network model's classification ability.

4.1 Experimental environment.

The experimental operating system is Windows 10, the CPU is Intel(R) Core(TM) i9-9900 CPU @ 3.60 GHz with 64GB of memory. An NVIDIA RTX 2080Ti graphics card is used to accelerate computations. The input image size is normalized to $224 \times 224 \times 3$. The program is written in Python relying on the deep learning open-source framework Tensorflow. The initial learning rate is set to 0.0001, Dropout is set to 0.5, batch size is 32, and epochs are 100.

4.2 Analysis of influence factors of model performance

Comparison of migration learning effect. Fig. 5 shows the accuracy curves with and without transfer learning. The validation set accuracy for the model combining VGG16 and transfer learning shows a higher accuracy and faster convergence speed than the baseline VGG16 model. The VGG16 + transfer learning model stabilizes at 35 epochs, while the VGG16 model only stabilizes at 62 epochs. Furthermore, the accuracy of the VGG16 + transfer learning model reached around 0.76, whereas the VGG16 model only reached about 0.7. This indicates that after using transfer learning, the network training precision is higher, the training speed is faster, and it can stabilize more quickly. The loss curves also show that the VGG16 model using transfer learning has less oscillation and is more stable.

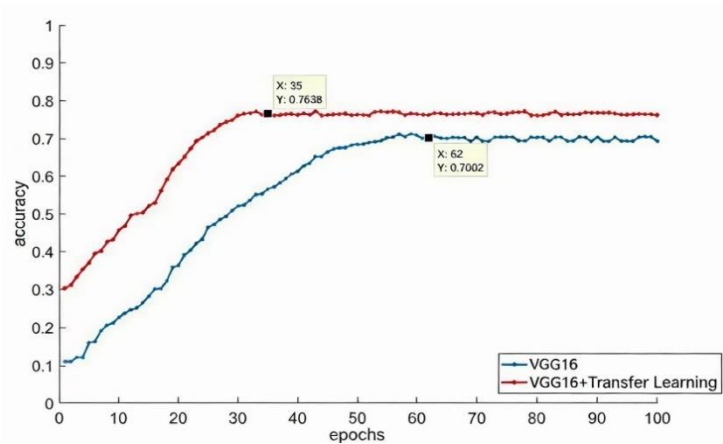


Figure 5. Relation Curve Of Iterative Times And Accuracy Rate Of Transfer Learning

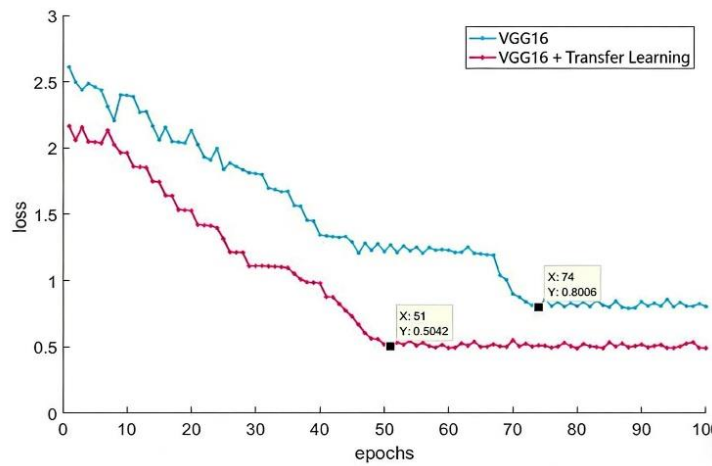


Figure 6. Relation Curve Of Iteration Number And Loss Value Of Transfer Learning

It can be seen from Fig. 6 that the accuracy rate on the verification set, compared with the VGG16 model, the model combined with VGG16 and migration learning has higher accuracy rate and faster convergence speed, and the image changes are more stable after stabilization. The VGG16+migration learning model tends to be stable when there are 35 s epoch, while the VGG16 model tends to be stable when there are 62 s epoch. This shows that the training accuracy of the network after using migration learning is higher, and the training speed is faster, and the network can be smoothed more quickly.

It can be seen from Fig. 6 that the vibration of loss curve appears in the training process of the original VGG16 network model, and the VGG16 network model with migration learning is used, which is small and more stable, indicating that the improved VGG16 network model is more stable, and the error reduction trend in the training process is accelerated and the accuracy rate is improved.

1) Comparison of multi-loss function fusion effect.

The results of comparison between the multi-loss function fused on the film damage classification data set and the common central loss function on classification accuracy are shown in Table 2.

Table 2 Comparison Of Classification Accuracy Of Each Loss Function On Film Damage Classification Data Set(%)

Loss function	Classification accuracy(%)
Cross entropy loss function	76.38
Center loss function	76.12
Multi-loss function fusion	76.61

Experimental results show that using multi-loss function fusion yields classification accuracies 0.25 and 0.49 percentage points higher than using cross-entropy or center loss functions alone. The value of the fusion coefficient α also impacts accuracy. As the fusion coefficient increases, classification accuracy gradually improves, peaking at $\alpha = 0.5$, and then gradually declines. Moderate fusion effectively improves classification accuracy.

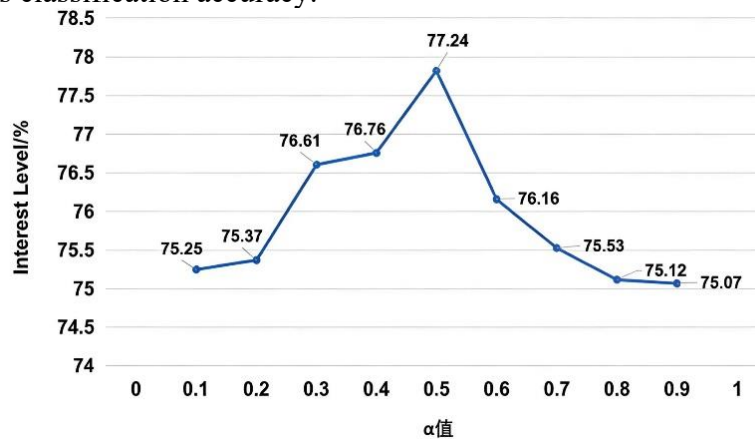


Figure 7. Effect Of Fusion Coefficient A on Classification Accuracy in Film Damage Classification Data Set

It can be seen from Fig. 7 that with the increase of fusion coefficient, the accuracy rate of classification in the image data set of film damage is gradually improved. When $\alpha = 0.5$, the accuracy rate of classification reaches the highest, and then gradually decreases. Experiments show that the cross-entropy loss function controls the trend of the model as a whole, and the center loss function can capture and learn the feature of smaller distance in the class.

2) Comparison of effect of BN layer.

When $\alpha = 0.5$, the accuracy comparison curves with and without the BN layer are analyzed. As can be seen from Fig. 8, the curve without the BN layer converges slower, gradually stabilizing at 32 epochs, whereas the model curve with the BN layer converges faster, having basically stabilized at 22 epochs. Experimental results show that after adding the BN layer to the model, the network model can utilize the mean and standard deviation on the mini-batch to make the parameters of the intermediate layers of the network obey the same distribution. This can accelerate the training and convergence speed of the network, prevent gradient explosion and gradient vanishing, and make the model more stable.

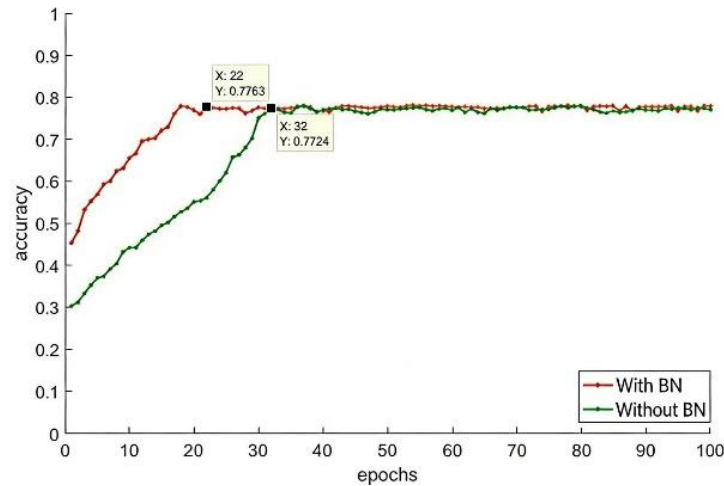


Figure 8. Relation Curve of Iterations and Accuracy Rate with or without BN Layer

4.3 Confusion matrix of film damage classification and identification results on BN-VGG16.

A confusion matrix can be used to visually display the performance of a classification model and is one of the important indicators for evaluating model results, commonly used to evaluate classifier models. This study involves 4 types of thin film damage categories. The improved BN-VGG16 model was used to conduct classification and recognition experiments on the test set data, and the resulting confusion matrix is shown in Fig. 9.

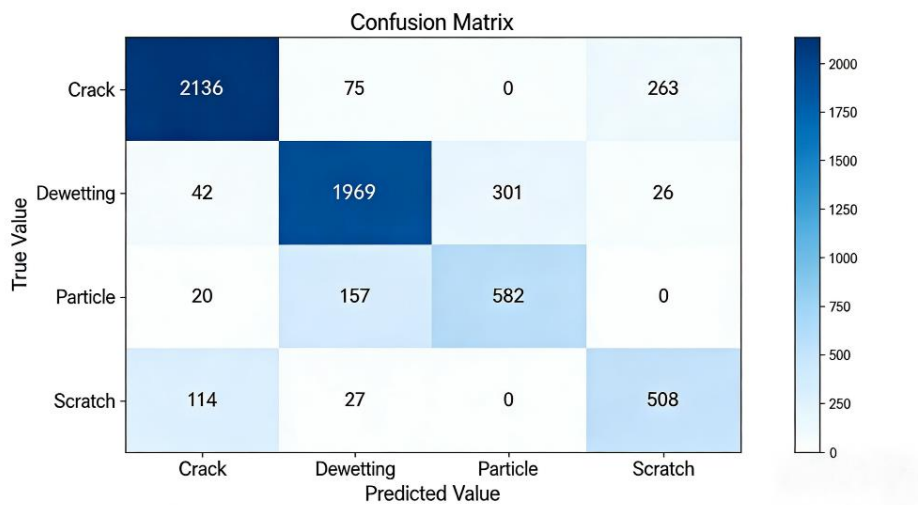


Figure 9. Mix Matrix of Film Damage Classification and Identification Results on BN-VGG16

Based on the confusion matrix, the accuracy, precision, recall, and F1 score of the model corresponding to each category can be calculated. The calculation results are shown in Table 3.

Table 3 BN-VGG16 Film Damage Classification And Identification Results Of Network Model

Damage category	Accuracy(%)	Accuracy(%)	Recall rate(%)	F_1 Score(%)
Cracks		92.15	86.34	89.15
Dehumidification	83.52	88.38	84.43	86.36
Particles		65.91	76.08	70.63
Scratch		64.22	78.27	70.55

As can be seen from Table 3, except for the precision and F1 score of scratches and particles, the others are all above 75%, and the precision of cracks has reached over 90%. The recognition precision, recall, and F1 score of particles and scratches are relatively low. The reason may be that the number of images of particles and scratches in the dataset is small, and the model did not learn the corresponding features well during the training process.

As can be seen from Fig. 9, 2136 crack images are recognized as cracks, 75 are recognized as dewetting, and 263 are recognized as scratches. Because some images of cracks and scratches are relatively similar, they are prone to recognition errors. The reason why cracks are recognized as dewetting is that the image background is relatively complex, causing the network to make recognition errors. 1969 dewetting images are recognized as dewetting, 42 are recognized as cracks, 301 are recognized as particles, and 20 are recognized as scratches. Because some images of dewetting and particles are relatively similar, they are prone to recognition errors. The reason for being recognized as cracks and scratches is the relatively complex background. 582 particle images are recognized as particles, 26 are recognized as cracks, and 157 are recognized as dewetting. 508 scratch images are recognized as scratches, 114 are recognized as cracks, and 27 are recognized as dewetting.

4.4 Ablation Experiment on BN-VGG16.

This section conducts ablation experiments on the self-made thin film damage image test set. Ablation experiments were performed for all possible scenarios of the BN-VGG16 model. Transfer learning, multi-loss function fusion, and the BN layer were sequentially added to the original model; multi-loss function fusion and the BN layer were sequentially added based on the original model and transfer learning; and transfer learning, multi-loss function fusion, and the BN layer were added to the original model. The experimental results are shown in Table 4.

Table 4 Ablation Experiment On Self-Made Film Damage Image Test Set

Original model	Migration learning	Multi-loss function fusion	BN layer	Accuracy(%)
√				70.02
√	√			76.38
√		√		71.39
√			√	72.01
√	√	√		76.82
√	√		√	76.59
√	√	√	√	77.63

As can be seen from Table 4, when transfer learning, multi-loss function fusion, and the BN layer are used on the basis of the original model, the accuracy of the model is improved by 6.36%, 1.37%, and 1.99%, respectively; when multi-loss function fusion and the BN layer are added sequentially on the basis of the original model and transfer learning, the accuracy of the model is also improved by 0.44% and 0.21%, respectively; when transfer learning, multi-loss function fusion, and the BN layer are added to the original model, the accuracy of the model improves the most, ultimately reaching a classification accuracy of 77.63% for thin film damage images.

The accuracy of the BN-VGG16 model for thin film damage image classification is not highly ideal. The accuracy is only 77.63%, which is far from the estimated value of the expected precision. Moreover, the BN-VGG16 model has a large number of parameters (over 10 million parameters) and a long training time, making it less suitable for later embedded development of the model. Therefore, this paper proposes a more lightweight convolutional classification network model, CBAM-ResNet50. Compared with VGG16, ResNet50 is a deeper network but has fewer parameters.

ResNet50 consists of 50 convolutional layers, which include residual blocks. These blocks reduce the number of parameters through direct cross-layer connections and can mitigate the gradient vanishing problem, making ResNet50 easier to converge during the training process and achieving higher model performance. Therefore, relatively speaking, ResNet50 is a more suitable lightweight model option for use under limited computing resources.

1) Comparison between this algorithm and existing algorithms.

To further prove the effectiveness of the algorithm, common models in image classification such as AlexNet, GoogLeNet, VGG16, VGG19, ResNet18, ResNet50, and ResNet101 were selected to conduct comparative experiments from three aspects: test set accuracy, training time, and parameter quantity. The specific experimental results are shown in Table 5.

Table 5 Film Damage Classification Performance Of Different Models

Model	Accuracy of test set(%)	Training time(H)	Parameter quantity
AlexNet	63.28	57	57.02×10^6
GoogLeNet	60.59	42	4.88×10^6
VGG16	70.02	135	130.38×10^6
VGG19	67.19	142	139.59×10^6
ResNet18	64.32	21	21.80×10^6
ResNet50	65.01	25	25.5×10^6
ResNet101	64.57	41	44.55×10^6
BN-VGG16	77.63	109	94.57×10^6

As can be seen from Table 5, the BN-VGG16 network model proposed in this paper achieved an accuracy of 77.63% on the test set, ranking first, although BN-VGG16 is slightly inferior to other networks in terms of training time and training parameters. The comparative results show that the BN-VGG16 network model has a high classification and recognition precision, indicating that the improved BN-VGG16 model has good performance and can be applied to the recognition of thin film damage types.

5. Summary

1) Through image collection, image preprocessing, and image augmentation, this study constructed a dataset of four damage types of thin films and applied the dataset to the constructed BN-VGG16 model. Using methods of transfer learning, multi-loss function fusion, and adding a BN layer to each convolutional layer improved the recognition rate of the convolutional neural network on this experimental dataset. The recognition rate of the proposed model is higher than that of traditional machine learning algorithms and other improved algorithms based on convolutional neural networks, reaching up to 77% .

2) The recognition accuracy of the BN-VGG16 network model for thin film damage images in the validation set reached 77.63%. Compared with the AlexNet, GoogLeNet, VGG16, VGG19, ResNet18, ResNet50, and ResNet101 models, the test set recognition accuracy improved by 14.35, 17.04, 7.61, 10.44, 13.31, 12.62, and 13.07 percentage points, respectively.

3) A confusion matrix was used to visually display the performance of the classification model. The overall recognition accuracy of the test set reached 83.44%. Except for the precision and F1 score of scratches and particles, the others are all above 75%, and the precision of cracks reached over 90%. This proves that the BN-VGG16 model is suitable for the recognition and classification of thin film damage images.

Acknowledgments

The authors wish to thank the cooperators. This research is partially funded by the National-level College Students' Innovation and Entrepreneurship Fund Project (202510702057) and (202510702002X).

References

- [1] Y.C. Li: Heilongjiang Science and Technology Information, Vol. (2017) No.02, p.14-15. (In Chinese)
- [2] S. Geng: Research on Laser Thin Film Damage Identification Method Based on Image Features (M.S., Xi'an Technological University, China 2019). p.1-100.
- [3] S.W. Zhang: Research on Key Technologies of Laser Damage Test for Photoelectric Materials (Ph.D., Changchun University of Science and Technology, China 2023). p.1-120.
- [4] S.L. Xiang: Research on Laser-induced Damage Photoacoustic Detection Based on PVDF Thin Film Sensor (M.S., Soochow University, China 2021). p.1-95.
- [5] Y.R. Huang: Research on Key Technologies of Rapid Measurement of Laser Damage Threshold of Optical Thin Films (Ph.D., Changchun University of Science and Technology, China 2022). p.1-110.
- [6] W.W. Hai: Research on Laser-induced Damage Identification Technology Based on Terahertz (M.S., Xi'an Technological University, China 2020). p.1-88.
- [7] P. Franca, S. Valeria, P. Federica and others: Journal of Applied Toxicology, Vol. (2023) No., p.1-10.
- [8] A. Fanizzi, G. Scognamillo, A. Nestola and others: Frontiers in Medicine, Vol. 9(2022) No., p.993395.
- [9] V. Allapakam, Y. Karuna: Soft Computing, Vol. 27(2023) No., p.11877-11893.
- [10] D. Provenzano, J.Y. Wang, S. Haji Momenian and others: International Journal of Radiation Oncology, Biology, Physics, Vol. 117(2023) No.2, p.S132.
- [11] F. Zhang, Q. Wang, A. Yang and others: Frontiers in Oncology, Vol. 12(2022) No., p.861-857.
- [12] Y.T. Li, Y.Y. Huang, P.F. Wang and others: Journal of Optoelectronics·Laser, Vol. 35(2024) No.01, p.41-50. (In Chinese)
- [13] X.J. Zhu: Modern Electronic Technique, Vol. 47(2024) No.01, p.74-77. (In Chinese)
- [14] M.C. Vittoria, M. Matteo, A. Aurelio and others: Investigative Ophthalmology & Visual Science, Vol. 64(2023) No.13, p.20-20.
- [15] J. Qiu, W.R. Liu, Z.Y. Cao and others: Journal of Yunnan Agricultural University (Natural Science), Vol. 34(2019) No.5, p.884-888. (In Chinese)
- [16] X.C. Wei: Analysis of Deep Learning: Principles of Convolutional Neural Networks and Visual Practice (Publishing House of Electronics Industry, China 2018), p.1-256.
- [17] W.H.L. Pinaya, S. Vieira, R. Garcia-Dias and others: Convolutional Neural Networks (Academic Press, Pittsburgh 2020), p.1-300.
- [18] Q. Bai, L. Huang, J.N. Chen and others: Journal of Software, Vol. 29(2018) No.4, p.1029-1038. (In Chinese)
- [19] X.S. Han, W. Lin: Microcomputer & Its Applications, Vol. 36(2017) No.21, p.54-56. (In Chinese)

- [20] X.N. Hou, H.C. Liu, W.Z. Hou: *Computer Systems & Applications*, Vol. 31(2022) No.07, p.172-178. (In Chinese)
- [21] Q.B. Liu, X.L. Li, K. Wang: *Journal of Beijing University of Technology*, Vol. 50(2024) No.02,p.140-151. (In Chinese)